J|A|C|S
COMMUNICATIONS

Published on Web 08/20/2002

Crystal Structure of a Genomically Encoded Fosfomycin Resistance Protein (FosA) at 1.19 Å Resolution by MAD Phasing Off the L-III Edge of Tl^+

Chris L. Rife,[†] Rachel E. Pharris,[†] Marcia E. Newcomer,[‡] and Richard N. Armstrong*,[†]

Departments of Biochemistry and Chemistry, Vanderbilt University, Nashville, Tennessee 37232-0146, and Departments of Biological Sciences and Chemistry, Louisiana State University, Baton Rouge, Louisiana 70803

Received May 13, 2002

The fosfomycin resistance protein (FosA) is a Mn(II)-dependent metalloenzyme that catalyzes the addition of glutathione (GSH) to the broad-spectrum antibiotic fosfomycin, **1**, rendering it inactive (Scheme 1).[1] The plasmid-encoded enzyme originally derived from resistant clinical isolates of Serratia has been extensively characterized biochemically and spectroscopically.[1,2] Evidence suggests that the Mn(II) center is directly involved in catalysis and that the enzyme requires the monovalent cation K^+ for optimal activity. However, the exact roles of the divalent and monovalent cations in catalysis remain to be elucidated.

Scheme 1

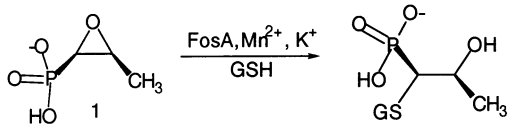

A survey of the microbial genome sequence database indicates that there are a number of FosA homologues encoded in the genomes of pathogenic microorganisms. These genes may confer an intrinsic resistance to the antibiotic and compromise its clinical efficacy. In this report, we describe the characterization and high-resolution structure of a protein that exhibits 60% sequence identity to the plasmid-encoded FosA but is encoded in the genome of the opportunistic pathogen *Pseudomonas aeruginosa*. The structure was solved exploiting the monovalent cation-binding site for multi-wavelength anomalous diffraction (MAD) phasing with thallium-(I).

The gene PA1129 was amplified from genomic DNA and ligated into a pET-20 expression plasmid. The protein expressed in BL21-DE3 *E. coli* cells confers robust resistance to fosfomycin. The purified enzyme has catalytic characteristics ($k_{cat} = 80 \pm 2\ s^{-1}$, $k_{cat}/K_M^{fos} = (2.1 \pm 0.1) \times 10^5\ M^{-1}\ s^{-1}$, and $k_{cat}/K_M^{GSH} = (1.20 \pm 0.09) \times 10^4\ M^{-1}\ s^{-1}$) similar to those of the plasmid-encoded FosA. Importantly, the enzyme is activated 15-fold by the monovalent cation K^+ with a $K_{act} = 10 \pm 2$ mM.[3]

FosA from *Pseudomonas aeruginosa* crystallized at 22 °C from 40% Pentaerythritol propoxylate 629[4] and 80 mM K_2HPO_4 (pH 7.0) in the presence 0.8 mM Mn^{2+} and 0.8 mM fosfomycin.[5] The structure was solved by MAD phasing off the thallium L-III absorption edge (12.658 keV) with a crystal soaked with thallium-(I) acetate. A three-wavelength thallium MAD data set at a resolution of 2.0 Å and a native data set to 1.35 Å resolution were collected at the Advanced Photon Source beamline 14BM-D. The thallium sites were located in difference Patterson maps and refined using the program SHARP.[6] The electron density map was improved by automated phase extension to the 1.35 Å native data, and 93% of the chain was traced with the unrestrained automated refinement procedure (ARP).[7] After initial model building in O[8] and refinement with REFMAC in the CCP4 program suite,[9] the refinement was completed in SHELXL[10] with anisotropic B-factors and the addition of riding hydrogen atoms. The R_{cryst} and R_{free} for the final model were 0.132 and 0.177, respectively.[11]

The protein fold, illustrated in Figure 1, is similar to that seen in structures of other members of the VOC superfamily, such as glyoxalase I or the extradiol dioxygenases, and consists of paired $\beta\alpha\beta\beta\beta$ motifs that form a cupped-shaped cavity for the metal ion binding site.[12] Like glyoxalase I, the metal sites exhibit a domain-swapped arrangement with one motif derived from each subunit. One unique feature of the structure is that β-strand-2 of the second $\beta\alpha\beta\beta\beta$ motif is truncated to help form the potassium ion binding loop between the second and third β-strands. A substantial part of the dimer interface includes an α-helix near the C-terminus that packs against the N-terminal $\beta\alpha\beta\beta\beta$ motif from the opposite subunit and a short C-terminal β-strand that interacts with the second β-strand of the same N-terminal motif.

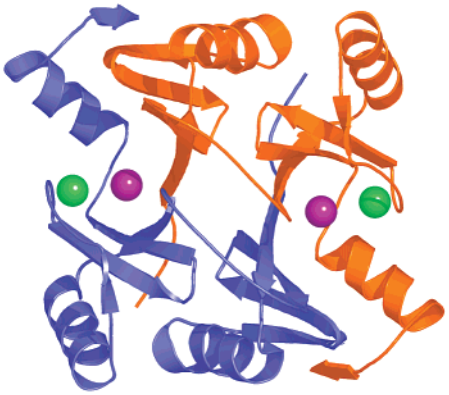

Figure 1. Ribbon diagram of FosA viewed down the noncrystallographic two-fold relating the two subunits. The positions of the Mn(II) and K^+ ions are shown as purple and green spheres, respectively. The image was created with the program PyMol.[13]

The protein ligands in the Mn(II) coordination site are H7, H64, and E110 as anticipated from sequence alignments and mutagenesis experiments.[1b,2a] Surprisingly, the Mn(II) is four-coordinate with a highly distorted tetrahedral geometry and a phosphate oxygen completing the inner-coordination sphere as illustrated in Figure 2.[14] Although a coordination number < 6 is anticipated on the basis of the large axial zero-field splitting in the EPR spectrum of the phosphate complex,[2c] four-coordinate Mn(II) is relatively rare in small molecule structures, and there are no examples in high-

* To whom correspondence should be addressed. E-mail: r.armstrong@vanderbilt.edu.
[†] Vanderbilt University.
[‡] Louisiana State University.

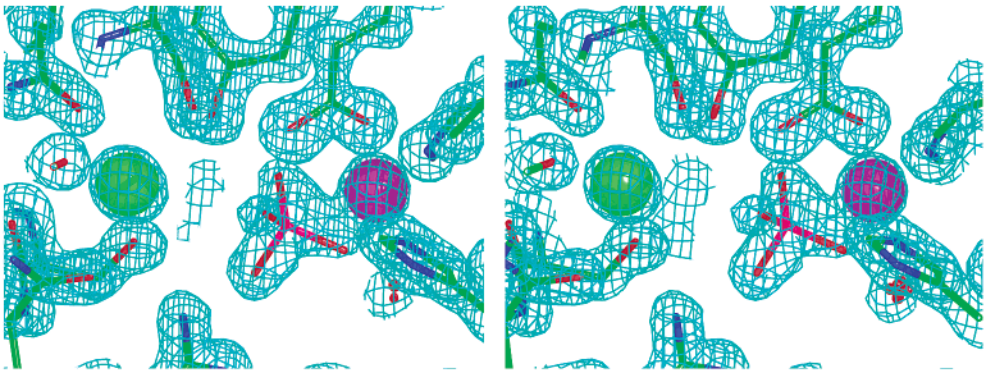

Figure 2. Divergent stereoview of the $2F_o - F_c$ (Φ_{calc}) electron density map at 1.35 Å resolution and contoured at 2σ near the Mn(II) site. The Mn(II) and K^+ ions are shown as purple and green spheres, respectively. The metal ligands clockwise from the top are E110, H64, H7, and the phosphate ion. The ligands are arranged in a highly distorted (flattened) tetrahedral geometry with the two histidines and the phosphate oxygen in the same equatorial plane.

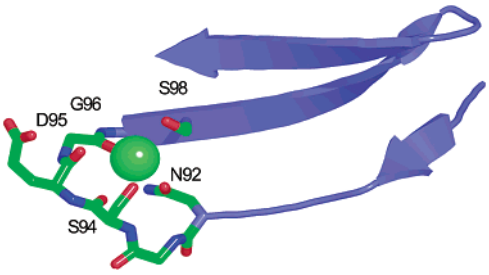

Figure 3. K^+ loop located between β-strands 2 and 3 of the second $\beta\alpha\beta\beta\beta$ domain. The five residues that contribute the six ligands to the coordination sphere are labeled.

resolution structures of proteins.[15] Although the crystals were obtained in the presence of fosfomycin, it is clear from the electron density maps that substrate is not in the coordination sphere of the metal due to the presence of phosphate in the buffer.

The potassium binding site, formed by an extended loop between two of the β-strands, is six-coordinate with four carbonyl oxygens and two serine hydroxyl groups serving as ligands (Figure 3). It is unusual in that there is no carboxylate ligand to the cation as is seen in most other K^+ binding loops.[16] The absence of a carboxylate ligand should enhance the electrostatic influence of the K^+ ion in the active site. The K^+ is located 6.5 Å from the Mn(II) ion, 4.4 Å from the carboxylate of E110, and 3.7 Å from the nearest phosphate oxygen.

To validate the use of Tl for MAD phasing of proteins that bind K^+, the structure of the thallium derivative was determined to 2.0 Å resolution. A rigid-body refinement of the native structure provided the initial model, and further adjustment of the model along with the addition of metal ions, water molecules, and ligands resulted in a final $R_{cryst} = 0.197$ and $R_{free} = 0.252$. A total of six Tl^+ sites are found in the asymmetric unit.[17] Of the four principal sites used to derive the experimental phases, two, as expected, are located in the K^+ binding sites (occupancy = 0.7), while the others (occupancy = 0.5) are located 7.1 Å away but just 3.8 Å from the Mn(II). The second set of sites is surprising because of the close proximity to the Mn(II) ion. Nevertheless, the second Tl site is chemically reasonable in that the metal is bound to the sulfur of C48 with two phosphate molecules bridging the Mn(II) and Tl ions (see Figure S2, Supporting Information). The presence of different types of Tl sites suggests that Tl may be more generally applicable for MAD phasing of protein structures, even those without K^+-specific sites. The L-III edge of Tl, which is at the same wavelength as the K-edge of Se, gives a strong anomalous signal at energies easily accessible at synchrotron light sources.

The structure of FosA in complex with fosfomycin was obtained from crystals soaked with a high concentration of the substrate. The structure was solved at a resolution of 1.19 Å by rigid-body refinement using the protein model from the phosphate complex. After adjustment of the model and the addition of the metals, we clearly observed electron density for fosfomycin near the Mn(II) site in a $F_o - F_c$ difference map (Figure 4). The final structural model was refined in SHELXL to a $R_{cryst} = 0.146$ and $R_{free} = 0.189$.

The substrate-bound structure reveals important details about the role of the Mn(II) and K^+ ions in catalysis. In contrast to the structure with the phosphate bound, the Mn(II) in this structure is very close to five-coordinate with nearly perfect trigonal bipyramidal geometry (Figures 4 and 5). The two histidines and one phosphonate oxygen occupy the coplanar equatorial sites, while

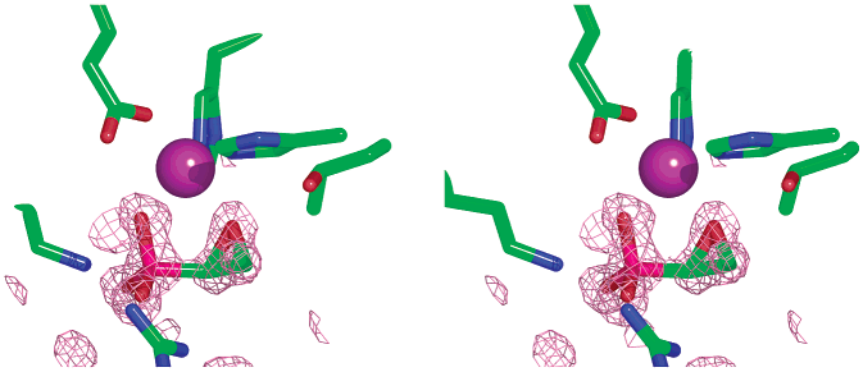

Figure 4. Divergent stereoview of the $F_o - F_c$ (Φ_{calc}) electron density of fosfomycin at 1.19 Å resolution contoured at 3σ. The difference map was generated before adding the substrate model and water molecules. The final refined model is shown in stick representation. The Mn(II) is shown as a purple sphere. The side chains shown clockwise from the top left are E110, H64, H7, T9, R119, and K90.

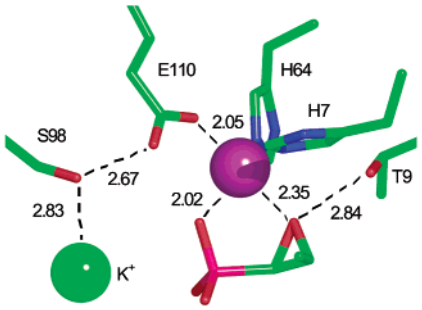

Figure 5. Potential sources of electrophilic catalysis in the active site of FosA. Internuclear distances between heteroatoms are given in Å. The Mn(II)−N bond distances for H64 and H7 are 2.12 and 2.11 Å, respectively.

the carboxylate of E110 occupies one of the apical sites. The oxirane oxygen of the substrate is located at the other apical site just 0.2 Å beyond the average Mn−O distance for five-coordinate Mn(II).[18]

The K^+ is located 4.4 Å from the nearest phosphonate oxygen and may contribute to the orientation of the substrate. The hydroxyl group of S94, which is part of the K-loop, forms a bridge between the K^+ and one of the phosphonate oxygens. Several other conserved residues are also within hydrogen bonding distance of the phosphonate oxygens, including the side chains of R119, K90, and Y100. The backside of carbon-1 of the substrate, to which GSH adds in the reaction, is located at the end of a short solvent channel near the surface of the protein. The residues that constitute the GSH binding site remain to be elucidated.

Importantly, the structure does reveal potential sources of electrophilic catalysis in opening the oxirane ring as illustrated in Figure 5. The most crucial of these involves the Mn(II) ion and the hydroxyl group of T9. The close proximity of the oxirane oxygen to the metal suggests that the Mn(II) stabilizes the alkoxide in a transition state perhaps via a true trigonal bipyramidal complex. The hydroxyl group of T9, which is conserved in the sequence of the plasmid-encoded enzyme, is positioned to act as a proton donor. Although the K^+ ion does not participate directly in catalysis, its influence may be relayed by the hydroxyl group of S98 (in the K-loop) which is within hydrogen bonding distance of E110 and thus in a position to enhance the electrophilicity of the Mn(II). Experiments to evaluate the mechanistic proposals herein and to determine the mode of interaction of GSH with the enzyme are underway.

Acknowledgment. This work was supported by NIH Grants R01 AI42756, P30 ES00267, and T32 GM08320. Use of the Advanced Photon Source was supported by the U.S. Department of Energy, Basic Energy Sciences, Office of Science, under Contract No. W-31-109-Eng-38. Use of the BioCARS Sector 14 was supported by the National Institutes of Health, National Center for Research Resources, under Grant No. RR07707.

Supporting Information Available: A description of the cloning of the gene, purification and characterization of the protein, data collection statistics, refinement protocols, and structure validation (PDF). This material is available free of charge via the Internet at http://pubs.acs.org.

References

(1) (a) Arca, P.; Rico, M.; Brana, A. F.; Villar, C. J.; Hardisson, C.; Suarez, J. E. *Antimicrob. Agents Chemother.* **1988**, *32*, 1552. (b) Bernat, B. A.; Laughlin, L. T.; Armstrong, R. N. *Biochemistry* **1997**, *36*, 3050.
(2) (a) Bernat, B. A.; Laughlin, L. T.; Armstrong, R. N. *Biochemistry* **1999**, *38*, 7462. (b) Bernat, B. A.; Armstrong, R. N. *Biochemistry* **2001**, *40*, 12712. (c) Smoukov, S. K.; Telser, J.; Bernat, B. A.; Rife, C. L.; Armstrong, R. N.; Hoffman, B. M. *J. Am. Chem. Soc.* **2002**, *124*, 2318.
(3) Experimental details are given in Supporting Information.
(4) Gulick, A. M.; Horswill, A. R.; Thoden, J. B.; Escalante-Semerena, J. C.; Rayment, I. *Acta Crystallogr.* **2002**, *D58*, 306.
(5) The enzyme crystallized in the orthorhombic space group $P2_12_12_1$ a = 54.79 Å, b = 66.97 Å, c = 77.00 Å, $\alpha = \beta = \gamma = 90°$ with a single dimer in the asymmetric unit.
(6) de La Fortelle, E.; Bricogne, G. *Methods Enzymol.* **1997**, *276*, 472. The experimental phases were obtained from four thallium sites (two per subunit) in the asymmetric unit. The sites were refined in Patterson space with occupancies of 0.5.
(7) Lamzin, V. S.; Wilson, K. S. *Methods Enzymol.* **1997**, *277*, 269.
(8) Jones, T. A.; Zou, J. Y.; Cowan, S. W.; Kjeldgaard, M. *Acta Crystallogr.* **1991**, *A47*, 110.
(9) Collaborative Computational Project, Number 4. *Acta Crystallogr.* **1994**, *D50*, 760.
(10) Sheldrick, G. M.; Schneider, T. R. *Methods Enzymol.* **1997**, *277*, 319.
(11) Details for data collection, refinement, and structure validation are given in Supporting Information. The crystallographic coordinates and structure factors for the phosphate-bound, Tl derivative and substrate-bound enzyme have been deposited in the Protein Data Bank under the file names 1LQK, 1LQO, and 1LQP, respectively.
(12) (a) Bergdoll, M.; Eltis, L. D.; Cameron, A. D.; Dumas, P.; Bolin, J. T. *Protein Sci.* **1998**, *7*, 1661. (b) Armstrong, R. N. *Biochemistry* **2000**, *39*, 13625.
(13) DeLano, W. L. The PyMOL Molecular Graphics System (2002) on World Wide Web http://www.pymol.org. The PyMOL program was used to generate Figures 1−5.
(14) The extra electron density about the metal is best explained with two partially occupied phosphate anions with slightly different orientations. There is no evidence of coordinated waters or other ligands to the metal. For clarity, only one phosphate is shown in Figure 2.
(15) (a) Bock, C. W.; Katz, A. K.; Markham, G. D.; Glusker, J. P. *J. Am. Chem. Soc.* **1999**, *121*, 7360. (b) Harding, M. M. *Acta Crystallogr.* **2001**, *D57*, 401.
(16) (a) Patterson, W. R.; Poulos, T. L. *Biochemistry* **1995**, *34*, 4331. (b) Larsen, T. M.; Benning, M. M.; Rayment, I.; Reed, G. H. *Biochemistry* **1998**, *37*, 6247. (c) McKay, D. B.; Sousa, M. C. *Biochemistry* **1998**, *37*, 15392. (d) Thoden, J. B.; Raushel, F. M.; Benning, M. M.; Rayment, I.; Holden, H. M. *Acta Crystallogr.* **1999**, *D55*, 8. (e) Harding, M. M. *Acta Crystallogr.* **2002**, *D58*, 872.
(17) The two sites not used in the initial phasing were refined with occupancies of 0.16 and 0.25.
(18) Palenik, G. J. *Inorg. Chem.* **1997**, *36*, 4888. The average Mn(II)−O bond distance for five-coordinate complexes containing only Mn−O bonds is 2.12 Å (1.99 Å min − 2.24 Å max).

JA026879V